Journal of Saudi Chemical Society (2022) **26**, 101433

King Saud University

Journal of Saudi Chemical Society

www.ksu.edu.sa
www.sciencedirect.com

ORIGINAL ARTICLE

Evaluation of adsorption and kinetics of neem leaf powder (*Azadirachta indica*) as a bio-sorbent for desulfurization of dibenzothiophene (DBT) from synthetic diesel

Olawumi Oluwafolakemi Sadare [a], **Augustine Omoniyi Ayeni** [b], **Michael Olawale Daramola** [a,*]

[a] *Department of Chemical Engineering, Faculty of Engineering, Built Environment and Information Technology, University of the Pretoria, Private Bag X20, Hatfield 0028, Pretoria, South Africa*
[b] *Department of Chemical Engineering, College of Engineering, Covenant University, Km. 10 Idiroko Road, Canaan Land, Ota, Nigeria*

Received 5 October 2021; revised 5 January 2022; accepted 17 January 2022
Available online 25 January 2022

KEYWORDS

Adsorbent;
Adsorption;
Diesel;
Dibenzothiophene;
Desulfurization;
Neem-leaf powder

Abstract The need for a sustainable environment has necessitated the development of a green adsorbent that is efficient, cheap, and readily available to serve as an alternative adsorbent for the removal of the refractory sulfur-containing compound from diesel. In this current study, neem-leaf powder (NLP) was activated using H_2SO_4 and tested in desulfurization adsorption experiments of synthetic diesel containing Dibenzothiopene (DBT) during a batch operation. The synthetic diesel contained 0.1 g of DBT in 100 mL of hexane. Before testing, physio-chemical characteristics of the adsorbent were checked via Fourier transmission infrared (FTIR) spectroscopy for surface chemistry; via N_2 physisorption at 77 K for textural properties; SEM quipped with EDX for morphology and elemental composition; and XRD for purity and crystallinity. The results showed that the physico-chemical nature of the adsorbent played a significant role in enhancing the adsorption capacity of the material for DBT. Activated NLP displayed DBT removal of 65.78% at 30 °C using 0.8 g of the adsorbent. Furthermore, the behaviour of the adsorbent during the adsorption could be adequately described using the Freundlich isotherm model. Pseudo-

* Corresponding author.
E-mail address: michael.daramola@up.ac.za (M.O. Daramola).
Peer review under responsibility of King Saud University.

Production and hosting by Elsevier

https://doi.org/10.1016/j.jscs.2022.101433

first-order and pseudo-second-order kinetics model describe well the adsorption kinetics of DBT onto the activated NLP.

1. Introduction

Energy production is one of the problems facing the world. Fossil-based sources, especially crude oil, are considered the major sources of energy. However, a major concern about the utilization of petroleum distillates such as diesel is the presence of sulphur compounds which when combust results in the emission of sulphur compounds into the atmosphere. The refining industry globally is facing new and more stringent environmental regulations on the minimum allowable sulphur content in diesel fuel [1]. Sulfur compounds are present in petroleum distillates in form of free sulphur, sulfides, disulfides, mercaptan, thiophene, benzothiophenes and dibenzothiophenes. During the direct combustion of diesel, sulfur oxides (SO_x) are released into the atmosphere, resulting in acid rain when SO_X reacts with moisture. In addition, it causes environmental pollution that is harmful to human health [1]. In view of these, urgent attention is needed to avoid the release of sulphur oxides into the environment, thereby preventing health-related issues.

To reduce sulfur content in diesel fuel, different existing techniques such as biodesulfurization (BDS), extraction, biochemical processes (EBP), oxidation, adsorption (ADS), and hydrodesulfurization (HDS) have been used with different levels of success. Among these desulfurization techniques, HDS is the most commonly used in the refineries [2] due to the efficacy of HDS to remove the sulphur-containing compounds such as thiols, thiolates, sulfoxides, and sulfones from diesel. However, operating HDS requires huge cost in terms of energy consumption because it if efficient only at very high temperature and pressure [3–5] and it does not remove many of the sulphur-containing aromatic compounds and long chains from the fuel at this condition, resulting into poor quality of fuel. [6–8]. In addition, the presence of these sulphur-containing aromatic compounds in the fuel reduces catalyst life and facilitates high consumption of hydrogen [9]. Furthermore, heterocyclic sulfur compounds such as dibenzothiophene (DBT) and its derivatives, especially 4,6-dimethyl dibenzothiophene (4,6-DMDBT), which constitutes about 70% of sulphur-containing compounds in diesel, cannot be removed HDS [10–12]. Therefore, research efforts should be channelled towards developing an efficient, readily available, and cheaper technique to remove DBT from petroleum distillate in an environmentally friendly way.

Recent research efforts have proposed the use of adsorption (ADS) for the removal of DBT from petroleum distillates. ADS is a promising and cost-effective option, because it can be operated at ambient temperature and pressure without using hydrogen and a catalyst [1,13–14]. Nitrogen-doped graphene (N-doped graphene) synthesized via chemical vapour deposition CVD has been employed as adsorbents for the removal of DBT from diesel [15]. However, from an environmental standpoint, the exploration of agricultural waste in the synthesis of adsorbents for DBT removal from diesel has emerged as sustainable development. Remarkably, from an economic point of view, agricultural waste materials are also inexpensive and readily available [16]. In this regard, several adsorbents, even from agricultural waste, have been proposed and tested for removal of DBT from petroleum distillates, thereby making the process more environmental benign [16]. Previous studies have reported the use of adsorbents obtained from rice husk, sawdust, pomegranate leaf powder and neem leaf powder for the removal of metal ions and organic pollutants from wastewater. As far as the authors of this article know, the use of neem leaf powder (NLP) as an adsorbent for removal of DBT from petroleum distillates has not been widely reported in the literature. Therefore, from this point of view, neem leaf powder, an agro-based waste, could be a promising material to use in the desulfurization of petroleum distillates because it is cheap and readily available, thereby proffering sustainable solution to desulfurization of petroleum distillates in an environmentally friendly way [17,18].

In addition, reports have shown that NLP has a wider range of useful products compared to other plants [19]. From literature, NLP has been explored as an adsorbent in the removal of pollutants and colour from water and industrial effluents. Padhare et al. [19] synthesized activated neem leave adsorbent using *ortho*-H_3PO_4 as an activating agent, however, only BET characterization was reported on it. Likewise, NLP was employed in a batch adsorption mode for effective detoxification of Congo Red (CR) and Methyl Orange (MO) from an aqueous solution in a study conducted by Ibrahim et al [20]. Sharma and Bhattacharyya [21] adsorbed Cadmium (Cd) ion, from aqueous solutions on NLP. Jinturkar and Sadgir [22] used neem leaf powder as an adsorbent for the removal of iron from an aqueous solution. Ahmaruzzaman and Gayatri [23] prepared an activated neem powder adsorbent using phosphoric acid. The synthesized adsorbent was used for removal of phenol, 4-nitro phenol, and 4-chlorophenol from an aqueous solution. Furthermore, NLP was used for the desulfurization of real diesel by Daware et al. [24]. However, there are little or no reports in the literature on adsorptive removal of DBT molecules, which account for about 70% of the sulfur organic compounds in diesel. Moreover, understanding behaviour of an adsorbent could be instrumental to designing and optimizing an adsorption process. Also, information on the nature of the interaction between adsorbate and an adsorbent is usually provided via an in-depth study of the adsorption behaviour of the material and its adsorption kinetics using existing isotherm models such as Langmuir and Freundlich isotherm and kinetic models such as Pseudo-first-order and Pseudo-second-order kinetic models [25]. Understanding this behaviour via the use of these models could provide information on the mechanism and the pathways of the adsorption interactions.

Against this background, this study, therefore, explores the application of neem leaf powder for removal of DBT is diesel and also provides information on the adsorption behaviour and kinetics of the adsorbent during the adsorption process.

2. Experimental

2.1. Materials

Neem leaf powder (NLP) was purchased from Organic choice (Ltd) South Africa, Dibenzothiophene (DBT), Acetonitrile (HPLC grade, 98%) and Hexane 98% were purchased from Sigma Aldrich Pty (Ltd), South Africa. All chemicals were used without further purification.

2.2. Preparation of activated NLP

Activating agent, H_2SO_4 was used on the as-received NLP to modify its surface morphology, thereby improving the physicochemical properties of NLP towards enhancing the adsorption capacity of the adsorbent as described elsewhere [26]. About 20 g of the as-received NLP was added into 10 mL of 0.5 M H_2SO_4. The mixture was stirred for 2 h at a temperature of 70 °C and allowed to dry in an oven at 110 °C. The sample was then carbonized in a furnace at 500 °C for 3 h. To remove the acid, the carbonized adsorbent was thoroughly washed with deionized water until a pH of 7 was attained, and dried at 70 °C in an oven for 24 h. The dried synthesized activated NLP was ground, sieved, and kept in a dry air-tight container until it was used in the adsorption experiment [26].

2.3. Characterization of activated NLP

The surface morphology of neem leaves powder was observed using CARL ZEISS sigma field electronic scanning electron microscope (FESEM) at different magnifications. The adsorbent was coated initially with 40% gold and 60% palladium (Au/Pd) before SEM analysis to avoid charge up. Elemental compositions of the adsorbent were checked by an Energy Dispersion X-ray (EDX).

The textural property of the adsorbent was determined by a micromeritics tristar 3000 static volumetric analysis unit via N_2 physio-sorption experiments at 77 K, to check the adsorbent's surface area, pore volume, and pore size. The Barret, Joyner, and Halenda (BJH) method was used to check the textural property (i.e. average pore size) of NLP before and after adsorption.

The surface chemistry of the adsorbent was checked by Fourier transform infrared (FTIR) spectroscopy using a Bruker Tensor 27 at a wavenumber range of 500–4000 cm^{-1} to determine the type of functional groups on the surface of the adsorbent samples. About 2 mg of the oven-dried powdered samples were mixed with 200 mg of potassium bromide (KBr), a spectroscopic material that allows transmission of IR. It was used as a carrier for the sample in this study to prevent interference in absorbance. The sample was pressed for 3 min at 20 MPa.

X-ray diffraction (XRD), using a Bruker D2 X-ray diffractometer, was used to identify the phases of the adsorbent. The measurement range was 20°–100° (2θ) and the observed phases were confirmed using EVA software with PLU2018-pdf-4-2018RDB database.

2.4. Performance evaluation of activated NLP

The performance evaluation of activated bio-sorbent NLP for desulfurization of sulphur compound (DBT) in model oil was conducted in batch mode, following the established experimental method described in the literature [27]. The best operating conditions and parameters were determined by varying the concentration of DBT, contact time, amount of adsorbent, and operating temperature during the batch adsorption experiments. To prepare the synthetic model oil, 0.1 g of DBT was dissolved completely in hexane (100 mL). Further dilutions were made from this solution to vary the concentration of DBT (250–1000 ppm). Time-dependent experiments were carried out for 180 min. Varied adsorbent amount (0.2–1.0 g) was added to 20 mL of model oil solution, each in an Erlenmeyer flask. The mixtures were thoroughly stirred on a digitally-monitored rotary shaker at 130 rpm, at three different temperatures (25–35 °C). Samples of desulfurized oil were taken and analyzed at 10 min intervals. All experiments were carried out in triplicates to reduce experimental error and ensure accuracy. The mean value of the data obtained was used in this study. To obtain a mathematical relationship, absorbance data of known concentration was obtained and used to plot the calibration curve. Then, the concentration of the unknown samples was determined from the pre-determined calibration curve. The adsorption capacity for each run of the experiments was determined using Eq. (1). The percentage removal was calculated using Eq. (2).

$$q_e = V\frac{C_i - C_f}{m} \tag{1}$$

$$\textit{Percentage removal}(\%) = \frac{\text{Initial DBT concentration} - \text{Final DBT concentration}}{\textit{Initial DBT concentration}} \times 100 \tag{2}$$

Where V is the volume of the model oil (L), m is the amount of adsorbent in g, C_i and C_f are the initial and final concentrations of DBT in the model oil in mg/L, respectively.

2.4.1. Analysis of desulfurized oil

Agilent High-Performance Liquid Chromatography (HPLC), Eclipse C-18 column was used to analyze the desulfurized model oil samples. N-Hexane was used as the mobile phase, at a wavelength of 280 nm, the flow rate at 1.0 µl/ min, and injection volume of 10 µl for 10 min.

2.5. Adsorption isotherms and kinetics

Freundlich and Langmuir isotherm models were used to analyze the equilibrium data in the adsorption experiment. The non-linearized Langmuir model is given in Eq. (3). The intercept and slope of the plot of $\frac{1}{q_e}$ *versus* $\frac{1}{C_e}$ from the linearized form of the Langmuir isotherm model in Eq. (4) were used to calculate the Langmuir constants b which is the reflecting affinity of binding sites and q_o (mg/g) is the maximum monolayer coverage capacities.

$$q_e = \frac{q_m b C_e}{1 + bC_e} \tag{3}$$

$$\frac{1}{q_e} = \frac{1}{q_o} + \frac{1}{bq_o C_e} \tag{4}$$

Where q_e is the amount of adsorbate in the adsorbent at equilibrium (mg/g) and C_e (mg/L) is the adsorbate equilibrium

concentration. The expression given in Eq. (5) was used to calculate the separation factor (R_L) to determine the favourability of the Langmuir adsorption process [25,28]

$$R_L = \frac{1}{1 + bC_o} \tag{5}$$

Where C_0 is the adsorbate initial concentration (mg/L), and b (L/mg) refers to the Langmuir coefficient [29]. The values of R_L between 0 and 1 indicate adsorption favourability, for an adsorption system under study, $R_L > 1$ represents unfavorable adsorption; $R_L = 1$ represents linear adsorption and $R_L = 0$ indicates irreversible adsorption.

Taking the logarithm of both sides of the Freundlich non-linearized model Eq. (6) gives Eq. (7). The intercept and slope of the plot of Log q_e versus log C_e of the linearized form of the Freundlich isotherm model in Eq. (7) were used to calculate the Freundlich constants K_f and n, relating to adsorption capacity (mg/g), and intensity of adsorption, respectively.

$$q_e = K_f C_e^{\frac{1}{n}} \tag{6}$$

$$Logq_e = LogK_f + \frac{1}{n} LogC_e \tag{7}$$

The magnitude of exponent $\frac{1}{n}$ indicates that the adsorption process is favourable.

Kinetic study on adsorption makes provision for important information on adsorption mechanisms and their reaction pathways. Lagergren pseudo-first-order kinetic model is the most useful and commonly recognized amongst the models [30]. Lagergren kinetic equation is given in Eq. (8):

$$\frac{dq_t}{q_t} = K_1(q_{e-}q_t) \tag{8}$$

After applying the boundary conditions of qt = 0 at t = 0, the integrated rate law gives;

$$Log(q_{e-}q_t) = Logq_e - \frac{K_1}{2.303} t \tag{9}$$

Where q_t is the amount of adsorbed DBT at time t and q_e is the amount of adsorbed DBT at equilibrium, K_1 (L/min) is the rate constant of the pseudo-first-order adsorption process. Adsorption rate constant K_1, can be calculated from a straight line graph obtained from the plot of log (q_e-q_t) versus t.

Ho and McKay pseudo-second order kinetics determines how the rate is dependent on the sorption capacity and not on the sorbate concentration [31]. The linearized form of second-order kinetics is given in Eq. (10):

$$\frac{t}{q_t} = \frac{1}{K_2 q_e 2} - \frac{1}{q_e} t \tag{10}$$

Where q_e is the amount of DBT adsorbed at equilibrium in (mg/L) and K_2 is the pseudo-second-order constant. The q_e and the K_2 are obtained from the slope and intercept of the plot of t/q_t versus t.

2.6. Re-usability of NLP during adsorption of DBT

For operation stability and re-usability of adsorbent, an impetus for commercial application, re-usability of NLP was evaluated. During the investigation, about 1.0 g of NLP (fresh) was mixed with 20 mL of solvent (hexane) containing DBT and was stirred at 40 °C at 130 rpm for 5 h. The amount of DBT adsorbed onto the NLP was recorded. Since hexane has a boiling point of 70 °C, therefore desorption was done at 40 °C to avoid operating at the boiling point of hexane. Therefore, adsorption and desorption formed a cycle. After complete desorption was achieved, the used NLP was used again with another fresh 20 mL of hexane containing DBT followed by desorption. The procedure was repeated 3 times after the first cycle, making 4 cycles. The initial and final concentrations of the solvent-containing DBT were analyzed by HPLC for each cycle to evaluate the % DBT removal for each cycle.

3. Results and discussion

3.1. Characterization of green activated NLP

Since the role of textural properties on the adsorption capacity of an adsorbent could not be overlooked, the textural characteristics of the NLP were checked. Textural properties such as surface area, pore volume, and pore sizes of the green adsorbents were determined by N_2 Physio-sorption experiments. Fig. 1 depicts the Barret, Joyner and Halenda (BJH) analysis showing the pore size distributions of activated NLP before, and after adsorption. Comparing the surface area of the adsorbent before and after adsorption, a decrease from 173.13 m^2/g to 153.60 m^2/g, respectively, was noticed. There was a decrease in the average pore size diameter from 34 nm (before adsorption) to 13.158 nm after adsorption, indicating that the material is mesoporous. The pore volume also decreased from 0.126 cm^3/g to 0.074 cm^3/g. These results agree with the previous results of Patel and Vashi [32] and Tsamo et al. [33].

Fig. 2 depicts the adsorption–desorption isotherm of the adsorbent. It could be seen that there was a wide gap between the adsorption and desorption isotherms, indicating that the pore condensation hysteresis has relatively weak attractive adsorbate-adsorbent interaction.

The FTIR spectra showing the functional groups in activated NLP before use and after use are shown in Fig. 3. The spectra indicated a peak at 1053 cm^{-1} attributable to the stretching of C-O functional groups [34]. The existence of carbonyl (C–O) stretching vibration of amide groups from plant protein is indicated by the band at 1622 cm^{-1}. The peaks at 1737 cm^{-1} could be assigned to the stretching vibration of carbonyl functional groups such as ketones, aldehydes, and carboxylic acids. The band at 2927 cm^{-1} indicates the existence of C–H stretching vibration of an aromatic aldehyde in neem powder, thereby confirming the report of Noorjahan et al. [35]. The result also shows that there was no chemical interaction between the adsorbent and the sulfur-containing compound in the synthetic oil.

Fig. 4 depicts the X-ray diffraction analysis of as-prepared neem leave powder. It is observed that there are no diffraction peaks except the band observed at 2-θ values in the range of 20°–30°. It can therefore be concluded that the adsorbent exhibits amorphous nature without any crystalline peaks, thereby confirming the report of Prabhu et al. [36].

SEM images of activated NLP before adsorption and after adsorption are shown in Fig. 5(a) and Fig. 5(b), respectively. Fig. 6a shows clearly that the pore structure of the adsorbent is of irregular surface structure. This structural state of the adsorbent could be instrumental to enhancing the adsorption of DBT because the adsorption of an adsorbent is a surface

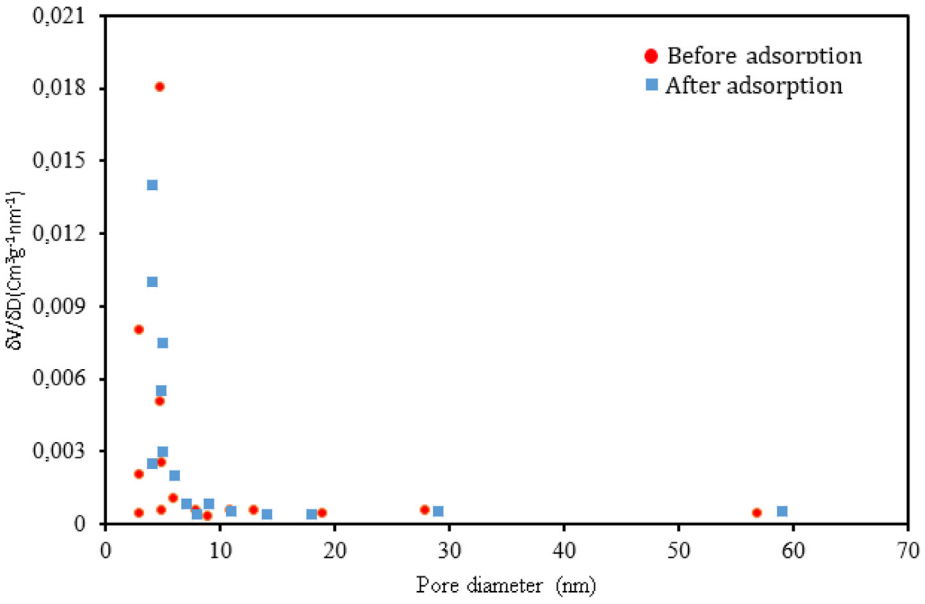

Fig. 1 BJH analysis for pore size distributions.

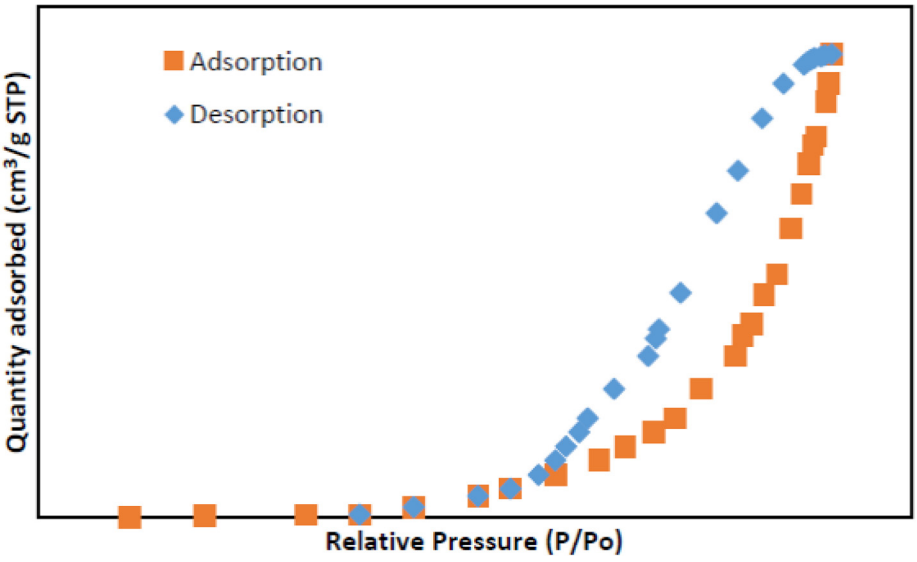

Fig. 2 Adsorption-desorption isotherm plot of NLP adsorbent.

phenomenon [37]. In addition, it could be observed that the surface morphology was rough before the adsorption of DBT onto the surface of the activate NLP. However, Fig. 5b showed a complete change in surface texture with smoother morphology. Interestingly, these results confirm findings from previous studies [38–40].

Fig. 6(A), Fig. 6(B), and Fig. 6(C) depict the EDX micrographs of the raw neem leave powder, (B) the activated neem leaves powder, and the neem leaves powder after adsorption, respectively. Additionally, Table 1 shows the elemental composition of the NLP before adsorption and after adsorption of DBT. It could be observed that as-prepared NLP consisted of a higher percentage of carbon and oxygen as compared to Mg, Cl, Ca and K that are insignificant [41]. Furthermore, the elemental composition of the NLP after desulfurization showed the presence of sulfur on the surface of the adsorbent.

3.2. Effect of adsorption conditions of performance of NLP adsorbent

Fig. 7 depicts the effect of contact time on desulfurization by activated NLP. The concentration (1000 mg/L), adsorbent amount (0.2 g), and temperature (30 °C) were kept constant at different time intervals. It could be observed that there was a rapid intake of DBT, thereby increasing the adsorption capacity of the adsorbent from 0 to 29.8 mg of DBT/g of the adsorbent, within the first 10 min. The initial higher adsorption rate observed at the early state of the adsorption process

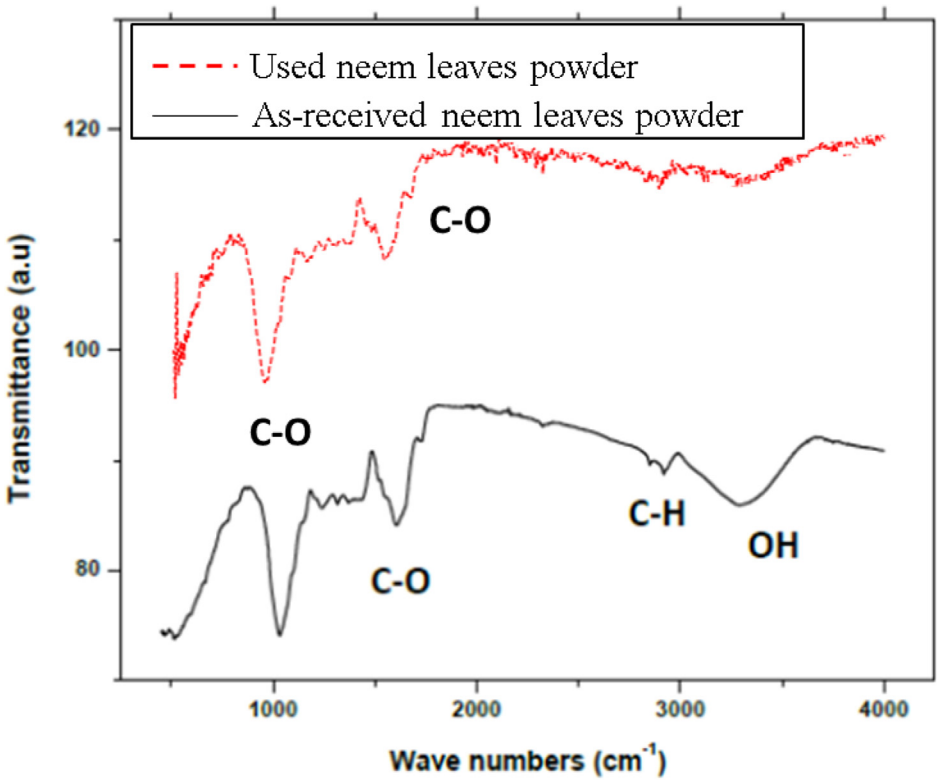

Fig. 3 Chemical functionalities of neem leaves powder before use and neem leaves powder after use.

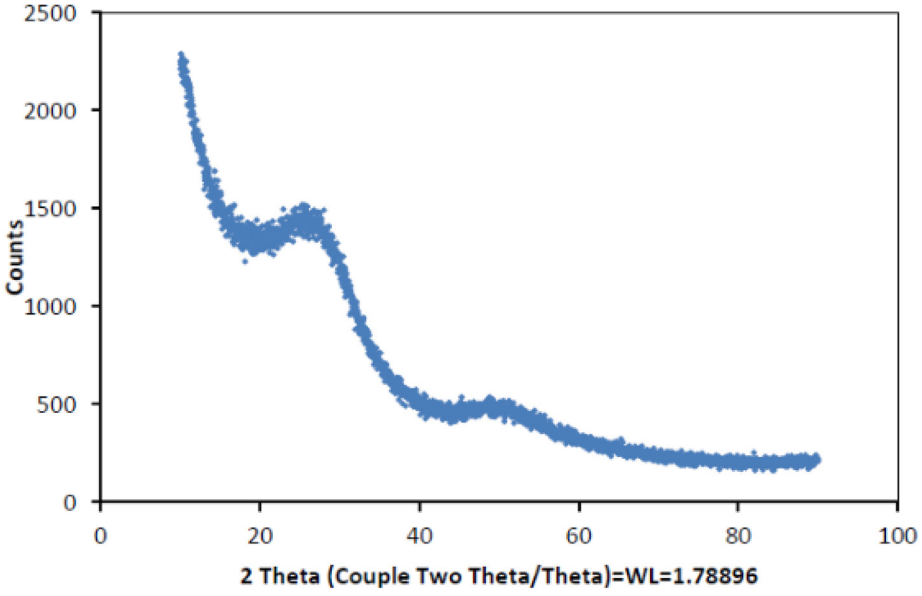

Fig. 4 XRD pattern of NLP adsorbent of the adsorbent at 2ɵ = WL = 1.78896.

could be attributed to the availability of more vacant sites on the surface of the adsorbent. However, as time proceeded, the uptake of DBT increased until it reached equilibrium at 39.8 mg/g [42]. Eventually, equilibrium was reached at 60 min when there was no further apparent increase in the adsorption capacity of the adsorbent. The single and continuous DBT adsorption curve obtained during the adsorption could be linked to the monolayer DBT coverage on the adsorbent surface as explained somewhere [43].

Fig. 8 explains the effect of temperature on adsorption using NLP. The results show that adsorption increased with an increase in temperature from 25 °C to 30 °C. The increase in adsorption with an increase in temperature may be attributed to the widening of pores of the adsorbent and some active

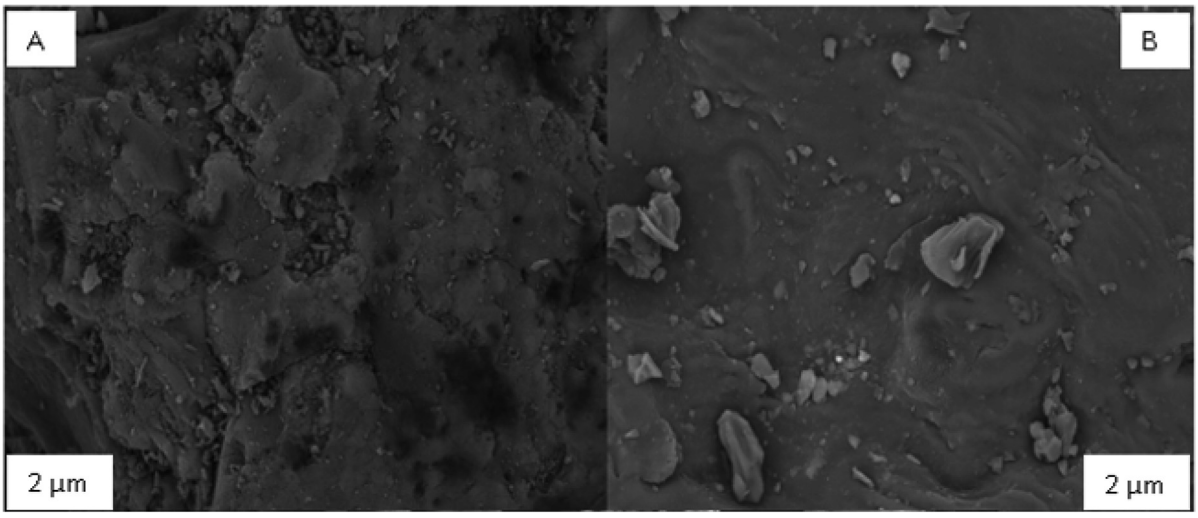

Fig. 5 SEM images of Neem powder (a) before adsorption (Magnification = 5.00 KX) and (b) after adsorption (Magnification = 5.00 KX).

site formation on the surface of the adsorbent due to bond cleavage at higher temperatures [44]. In addition, the observed behaviour at higher temperatures could be attributed to the increase in diffusion rate in the pore of the adsorbent due to an increase in temperature [45]. However, as the temperature increased from 30 °C to 35 °C, there was a decrease in the adsorption capacity of the adsorbent. This could be attributed to the fact that the adsorption process is exothermic. Furthermore, it may be attributed to the tendency of DBT molecules to escape from the solid phase to the bulk phase with the increasing temperature of the solution. Hence the highest adsorption capacity was obtained at 30 °C. This observation agrees with the findings in the literature [32,46].

Fig. 9 depicts the effect of the amount of adsorbent on the adsorption capability of activated NLP. It could be observed that, as the amount of adsorbent increased from 0.2 g to 0.8 g, the percentage of DBT removal from the model oil by NLP also increased. This may be due to the availability and accessibility of more adsorption sites and more surface area for sulfur compound attachment upon which the adsorption process is dependent [24,47–48]. However, there was no visible increase in adsorption capacity of the NLP when the amount of adsorbent increased from 0.8 g to 1.0 g, attributable to an increase in viscosity and inhibition of diffusion of DBT molecules to the surface of the activated NLP [49–51]. Therefore, a minimum amount (0.8 g) of the NLP could be appropriate for commercial application.

3.3. Effect of DBT concentration on the feed stream

Fig. 10 represents the effect of the concentration of desulfurization experiment. The initial DBT concentrations ranged from 250 to 1000 mg/L. Other operating conditions such as; contact time (60 min), temperature (30 °C), adsorbent amount (0.8 g), and volume of model oil (20 mL) were kept constant The results showed that the percentage removal of DBT increased from 43.4% to 51.0% with increasing initial DBT concentration from 250 to 1000 mg/L. An increase in DBT adsorption per unit mass of adsorbent from 2.71 mg/g to 12.76 mg/g with an increasing DBT concentration from 250 to 1000 mg/L, could be observed. This trend may be due to the concentration gradient developed at the surface of the adsorbent and the DBT solution which is as a result of increased mass transfer driving force. The findings in this study agree with the results obtained by Ishaq et al. [45].

3.4. Adsorption isotherms, the kinetics of NLP

Fig. 11(A) and 11(B) depict the Freundlich and Langmuir isotherm for activated NLP. Langmuir and Freundlich's isotherm parameters for adsorption of DBT molecules onto activated NLP adsorbent are given in Table 2. It can be observed that the adsorption of DBT onto the surface of activated NLP adsorbents was well described by the Freundlich isotherm model with higher coefficients of determination, R^2 (0.988). Although, coefficient of regression for Langmuir isotherm is 0.985, however, the straight line did not pass through the origin and the slope was negative. Therefore, it was not considered to describe well the adsorption of DBT molecules onto the adsorbent. The value of adsorption intensity, $n < 1$ for NLP shows favourability of the adsorption process.

Table 3 shows the parameters for pseudo-first-order and pseudo-second-order kinetics of DBT adsorption onto activated NLP. Comparing the coefficient of determination (R^2) of the kinetic models of activated NLP adsorbent, the correlation coefficients were higher in pseudo-second-order kinetics (0.9992, 0.9991 and 0.9989) than in pseudo-first-order kinetics (0.8349, 0.8857, and 0.857) at 298, 303 and 308 K, respectively. The kinetic model value for q_e calculated (37.46 mg/g) for psedo-second-order kinetics was very close to the experimental value obtained for q_e (38.46 mg/g). However, the model value calculated for q_e (38.46 mg/g) for pseudo-first-order kinetics, was lower than the value obtained in the experiment (10.69 mg/g). It could be assumed that the adsorption rate is controlled by the movement of DBT molecules in the pores of the activated green adsorbent. The same observation was reported by Wang and Wei [25]. The lower correlation coefficient factor for pseudo-first-order could be attributed to the

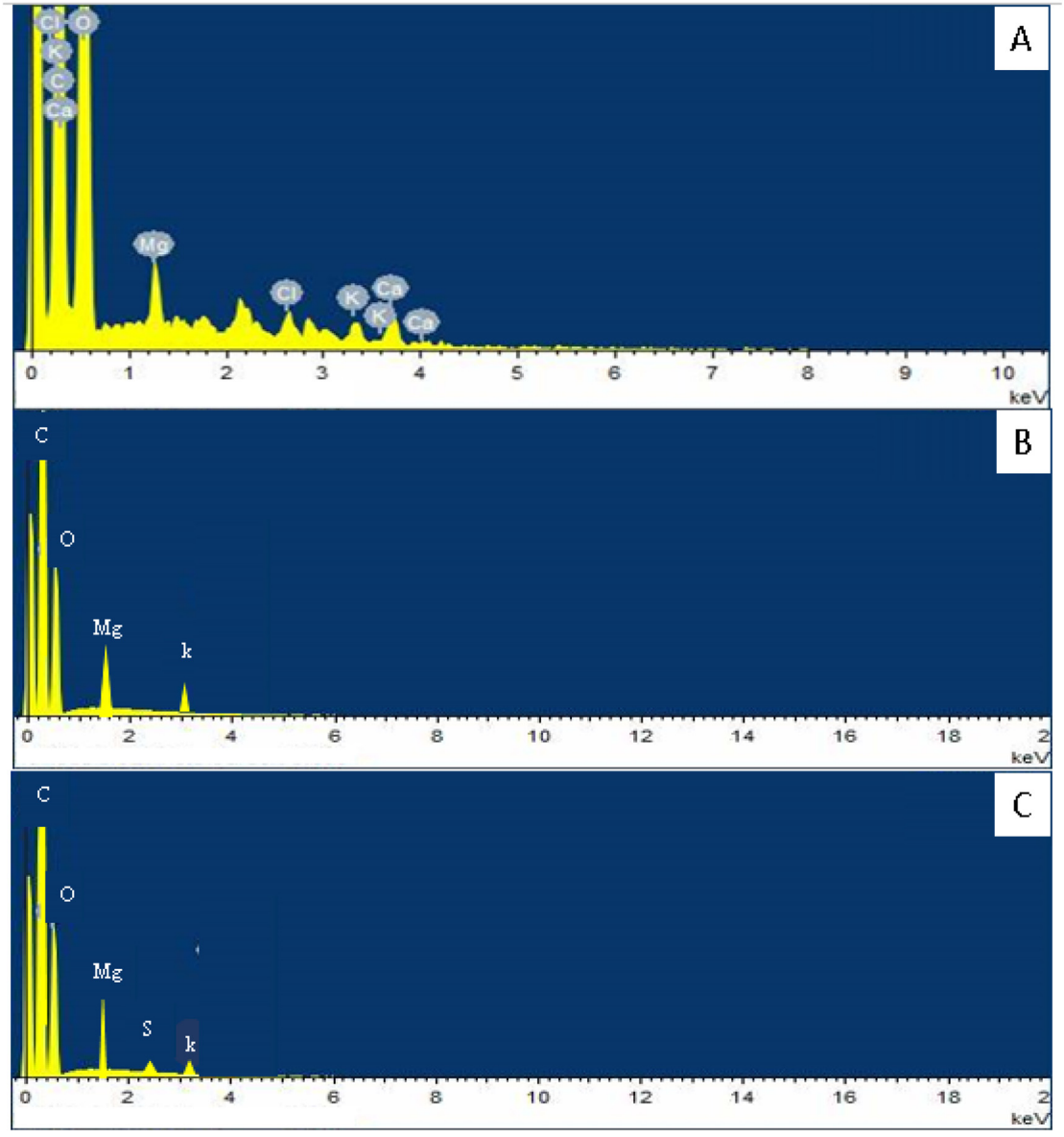

Fig. 6 EDX graph of (A) Raw neem leave powder (B) Activated neem leave before adsorption (C) Activated neem leave powder after adsorption.

Table 1 Elemental compositions of fresh NLP, activated neem NLP and used neem NLP as determined by EDX.

Element	Weight %			Atomic %		
	Fresh NLP	Activated NLP	Used NLP	Fresh NLP	Activated NLP	Used NLP
C	52.40	60.04	59.63	51.40	59.79	61.10
O	42.36	34.10	32.19	42.06	37.40	35.00
Mg	1.12	0.00	0.00	1.01	0.00	0.00
Cl	1.02	0.00	0.00	0.92	0.00	0.00
Si	0.00	5.86	3.71	0.00	2.81	3.01
K	1.25	0.00	0.00	0.85	0.00	0.00
Ca	1.85	0.00	0.00	1.25	0.00	0.00
S	0.00	0.00	2.51	0.00	0.00	0.89
Total	100.00	100.00	100.00	100.00	100.00	100.00

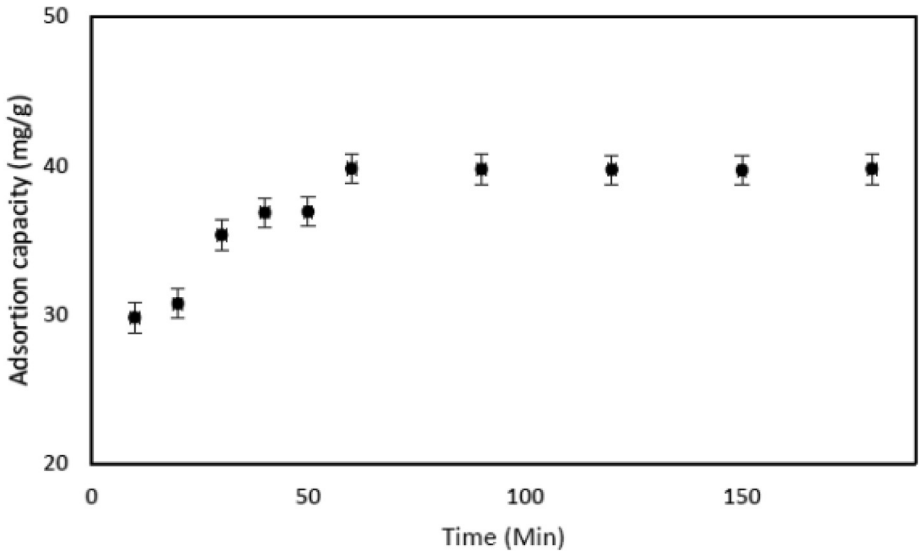

Fig. 7 Effect of contact time on desulfurization by neem leaves powder. Experimental conditions: Temperature: 30 °C; Adsorbent amount: 0.2 g; Initial DBT conc.:1000 mg/L.

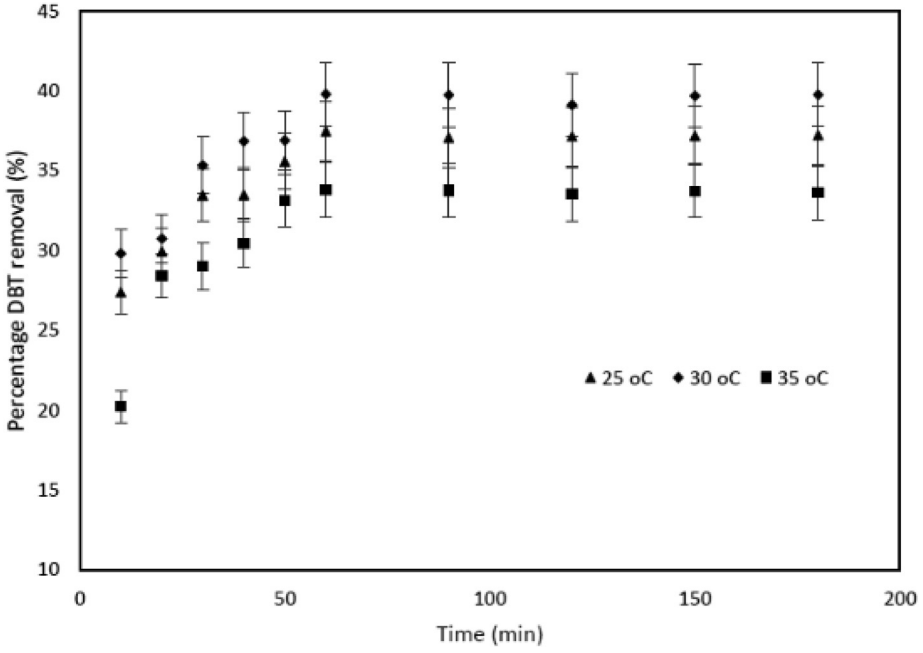

Fig. 8 Effect of temperatures on desulfurization of model oil. Experimental conditions: Adsorbent amount: 0.2 g; Initial DBT conc.: 1000 mg/L; varying temperatures: 25 °C, 30 °C and 35 °C.

fact that the rate of adsorption process is dependent on both concentration and time and not on the concentration factor. This result agrees with the findings of Kumar and Tamilarasan [52].

3.5. Re-usability of NLP during DBT adsorption

For operation stability and re-usability of adsorption, an impetus for commercial application, re-usability of NLP was evaluated. Fig. 12 depicts the re-usability cycles of activated NLP adsorbent. The results showed that adsorbent still retained its performance capacity until the 4th cycle. The DBT removal performance of the NLP decreased by 7.96% after the fourth cycle. This could be as a result of the blocked adsorption sites by DBT after repeated use of the adsorbent. However, the observation indicates that NLP can be re-used four times before it slightly loses its efficacy of efficiently removing sulphur compound from model oil.

Table 4, summarises the comparison of this study with previous studies in the literature. Daware et al. [24] employed NLP to remove sulfur-containing compounds from diesel oil with an adsorption capacity of 65% at an initial concentration of 250 µg/L (0.25 mg/L). However, in this study, same adsorbent was used, but model oil was employed. The results in this

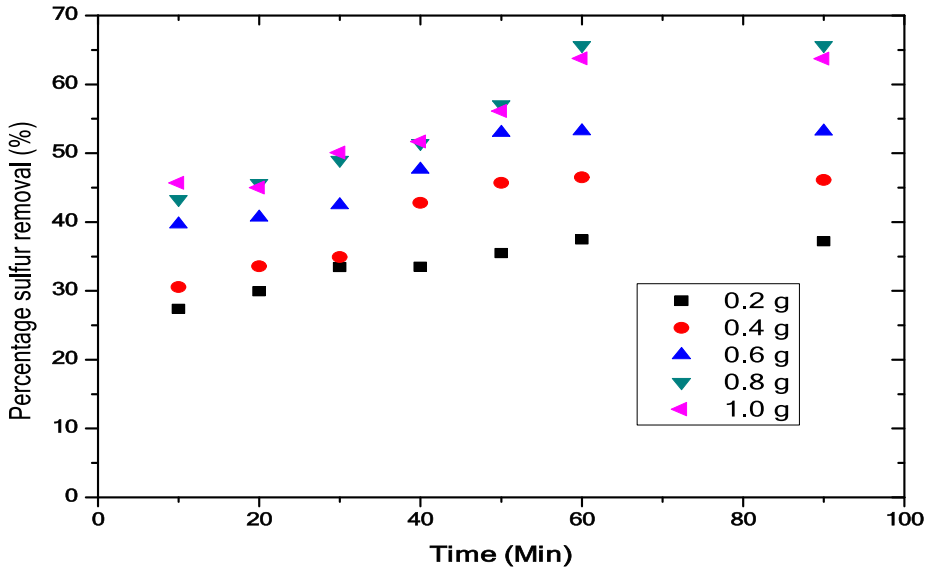

Fig. 9 Effect of adsorbent amount on desulfurization of model oil. Experimental conditions: Temperature: 30 °C.; Initial DBT conc.: 1000 mg/L at varying adsorbent amount.

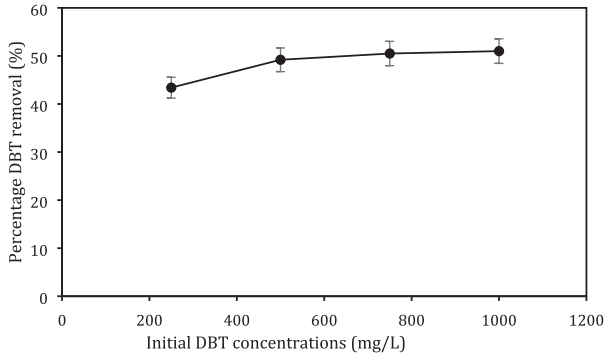

Fig. 10 Effect of initial concentration on adsorption of DBT. Experimental conditions: Contact time: 60 min; Adsorbent amount: 0.8 g; Temperature 30 °C.

recent study showed the same percentage removal of DBT by the adsorbent, although the initial DBT concentration in this current study is 75% higher than 0.250 mg/L used by Daware et al. [24]. This means the result obtained in this study is better when compared to the report of Daware et al. [24]. However, the effect of impurities (other compounds) present in real diesel could have contributed to the low DBT removal reported by the authors as against the model oil (pure DBT mixture) used in this study. Nazal et al. [41] impregnated about 15% Ni on activated carbon (AC) and carbon nanotubes (CNTs) to remove DBT from model oil. The results showed DBT removal of 76.4% and 43.4% respectively, for impregnated AC and impregnated CNTs. Comparing their results with the results of this study, it is obvious that the impregnated activated carbon of Nazal et al. [41] out-performed the NLP used in this study (65% DBT removal in this study as against (76.4% DBT removal in Ref. [41]. The better performance of

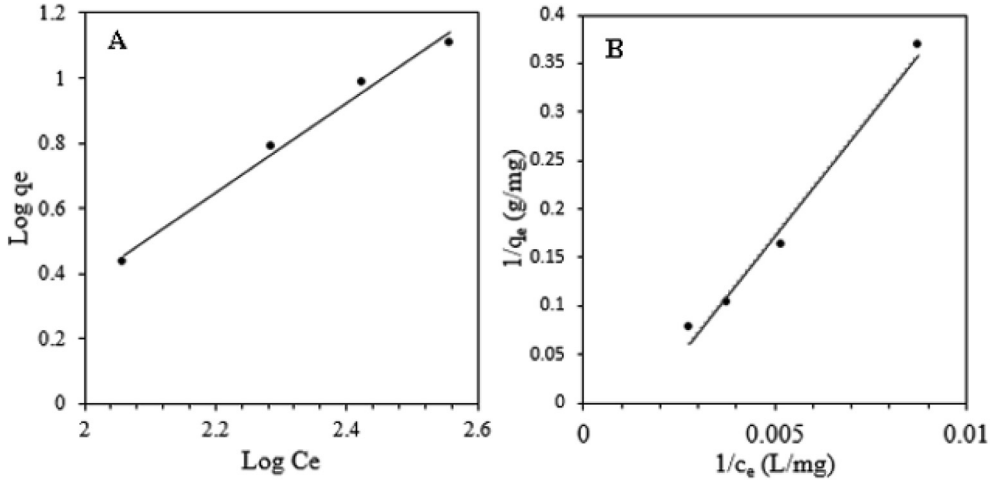

Fig. 11 Isotherm models for NLP (A) Freundlich (B) Langmuir. Experimental conditions: Initial DBT concentrations: 250–1000 mg/L; Temperature: 303 K, Amount of adsorbent: 1.0 g.

Table 2 Langmuir and Fruendlich isotherm parameters.

Adsorbents	Langmuir Isotherm				Freundlich Isotherm		
	Temp (K)	R_L	b (L/mg)	R^2	K_f (mg/g)	n	R^2
NLP	303	0.4	0.0015	0.985	0.0044	0.732	0.988

* b: Langmuir's constant, reflecting the activity of the binding site; K_f: Freundlich's constant; n:adsorption intensity; R: coefficient of determination; R_L: Langmuir separation factor.

Table 3 Kinetic model parameters for pseudo first and pseudo second order adsorption mode for NLP.

Temp (K)	Pseudo-1st-order (NLP)				Pseudo-2nd-order (NLP)			
	$q_{e(expt)}$ (mg/g)	$q_{e(calc.)}$ (mg/g)	K_1 (L/min)	R^2	$q_{e\ (expt)}$ (mg/g)	$q_{e\ (calc.)}$ (mg/g)	K_2 (g/mg.min)	R^2
298	38.46	10.69	0.0026	0.8349	38.46	37.46	0.0082	0.9992
303	39.80	14.78	0.0380	0.8857	39.80	39.80	0.0071	0.9991
308	33.80	6.76	0.0280	0.857	33.80	33.80	0.0078	0.9989

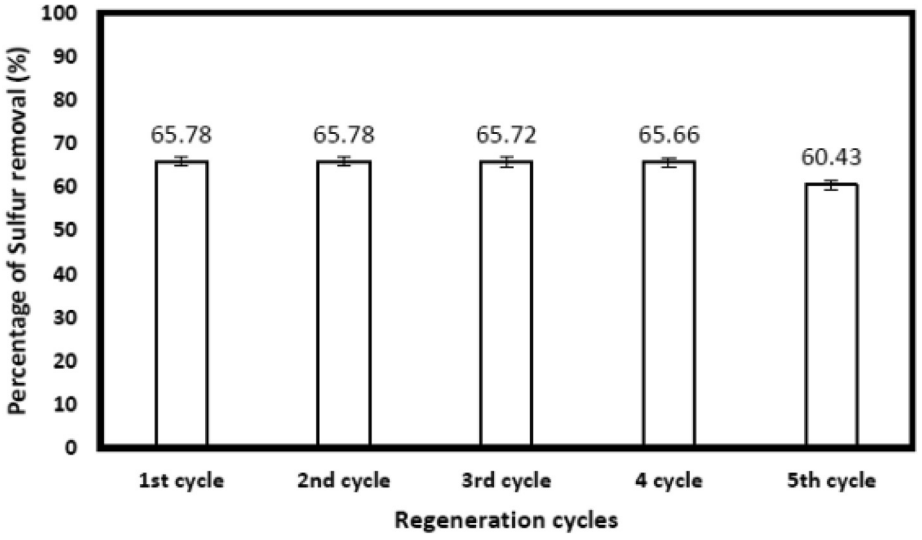

Fig. 12 Re-usability cycles of activated NLP adsorbent. Experimental conditions: Amount of adsorbent: 1.0 g; Volume of model oil: 20 mL; Initial DBT conc.: 1000 mg/L; Contact time: 60 min; Temperature 40 °C.

Table 4 Results compared with Literatures.

Adsorbent	Model oil	Initial conc. (mg/L)	Final conc. (mg/L)	% SR	Temp (°C)	Time (h)	Ads. Dosage (g)	Volume of diesel (mL)	Refs.
Neem leaves	Diesel	0.25	0.1	65.0	20	3.5	2.00	10	[23]
AC/15Ni	DBT	250	59.0	76.4	25	2.0	0.15	25	[39]
CNTs/15Ni	DBT	250	141.5	43.4	25	2.0	0.75	25	[39]
Zn-MMT	DBT	1000	190.0	81.0	25	1.0	1.50	20	[46]
Neem leaves	DBT	1000	342.2	65.8	30	1.0	0.80	20	This study

Zn-MMT: Zinc impregnated on montmorollonite clay.

their activated carbon could be attributed to the higher surface area of the activated carbon. However, it is noteworthy to mention that the initial DBT concentration of 250 mg/L used in Ref. [41] is 75% lower than the one used in this current study. Furthermore, the DBT removal of NLP in this study out-performed that of the Ni-impregnated CNTs reported in Ref. [41]. Furthermore, Zinc impregnated on MMT clay was reported by Ahmad et al. [47] for removal of DBT from model oil. Their findings showed that Zn-MMT was able to achieve 81% desulfurization at 25 °C, and at an initial DBT concentration of 1000 mg/L, making this adsorbent display better performance than the NLP investigated in this study. However, it is noteworthy to indicate that 1.5 g of adsorbent was used in Ahmad et al. [47] as against the 0.8 g used in this study. Nevertheless, the adsorption performance of NLP investigated in this study could be enhanced by enhancing its surface area via modification with metal. Therefore, it cannot be inferred that the adsorbent investigated in this study is capable of removing DBT at a higher initial concentration.

4. Conclusion

The need for a cleaner environment has necessitated the development of a green adsorbent that is cheap and readily available to serve as an alternative adsorbent for the removal of the refractory sulfur-containing compound from diesel. Activated NLP was successfully synthesized in this study. The SEM images of the activated NLP showed clearly that the pore structure of the adsorbent is of irregular surface structure. This could be instrumental to the performance of the NLP for the adsorptive removal of DBT from model diesel. The 65.78% removal of DBT from diesel (as indicated by the model oil) showcased the efficacy of activated NLP as a promising adsorbent. The NLP can be of great value in commercial application since its re-usability is promising. In addition, the Freundlich isotherm model describes well the adsorption behaviour of the DBT onto the activated NLP adsorbent and pseudo-first-order and pseudo-second-order kinetics describe well the adsorption kinetics of DBT onto the activated NLP.

From environmental and economic point of view, NLP, an agricultural waste materials could serve as a sustainable material (adsorbent) for adsorption of DBT from petroleum distillate. Thus, the results documented in this article could serve as a proof of concept and also as a platform upon which further research efforts could be built.

CRediT Author statement

Olawumi Oluwafolakemi Sadare: Conceptualization, Data curation, Formal analysis, Writing-original draft, Writing-review & editing. **Augustine Omoniyi Ayeni:** Writing-review & editing. **Michael Olawale Daramola:** Conceptualization, Project administration, Writing-review & editing.

Declaration of Competing Interest

The authors declare that they have no known competing financial interests or personal relationships that could have appeared to influence the work reported in this paper.

Acknowledgements

The authors hereby acknowledge the financial assistance of L'Oréal-UNESCO foundation for Women in Science, Sub-Saharan African Fellowship provided OOS for her Ph.D. degree program.

References

[1] Y. Yang, H. Lu, P. Ying, Z. Jiang, C. Li, Selective dibenzothiophene adsorption on modified activated carbons, Carbon 45 (2017) 33042–33059.
[2] R. Javadli, A. de Klerk, Desulfurization of heavy oil, Applied Petrochemical Research 1 (1-4) (2012) 3–19.
[3] B.L. McFarland, Biodesulfurization, Curr. Opin. Microbiol. 2 (3) (1999) 257–264.
[4] M. Rashtchi, G.H. Mohebali, M.M. Akbarnejad, J. Towfighi, B. Rasekh, A. Keytash, Analysis of biodesulfurization of model oil system by the bacterium, strain RIPI-22, Biochem. Eng. J. 29 (3) (2006) 169–173.
[5] S. Rashidi, M.R. Khosravi Nikou, B. Anvaripour, Adsorptive desulfurization and denitrogenation of model fuel using HPW and NiO-HPW modified aluminosilicate mesostructures, Microporous Mesoporous Mater. 211 (2015) 134–141.
[6] B.R. Folsom, D.R. Schieche, P.M. DiGrazia, J. Werner, S. Palmer, Microbial desulfurization of alkylated dibenzothiophenes from a hydrodesulfurized middle distillate by *Rhodococcus erythropolis* I-19, Appl. Environ. Microbiol. 65 (1999) 4967–4972.
[7] D.J. Monticello, Riding the fossil fuel biodesulfurization wave, Chem. Technol. 28 (1998) 38–45.
[8] J. Sharaf, Exhaust emissions and its control technology for an internal combustion engine, Int. J. Eng. Res. Appl. 3 (4) (2013) 947–960.
[9] H. Mei, B.W. Mei, T.F. Yen, A new method for obtaining ultra-low sulfur diesel fuel via ultrasound assisted oxidative desulfurization, Fuel 82 (2003) 405–414.
[10] Z. Ismagilov, S. Yashnik, M. Kerzhentsev, V. Parmon, A. Bourane, F.M. Al-Shahrani, A.A. Hajji, O.R. Koseoglu, Oxidative desulfurization of hydrocarbon fuels, Catal. Rev.: Sci. Eng. 53 (2011) 199–255.
[11] M. Ja'fari, S.L. Ebrahimi, M.R. Khosravi-Nikou ,Ultrasound-assisted oxidative desulfurization and denitrogenation of liquid hydrocarbon fuels: A critical review. Ultrason. Sonochem., 40 Part A, (2018) 955-968.
[12] M. Mohammadian, M.R. Khosravi-Nikou, A. Shariati, M. Aghajani, Model fuel desulfurization and denitrogenation using copper and cerium modified mesoporous materials (MSU-S) through adsorption process, Clean Technol. Environ. Policy 20 (1) (2018) 95–112.
[13] H.S. Bamufleh, Adsorption of dibenzothiophene (DBT) on activated carbon from Dates' Stones using phosphoric acid (H_3PO_4), JKAU Eng. Sci. 22 (2) (2011) 89–105.
[14] M. Ahmadi, B. Anvaripour, M.R. Khosravi-Nikou, M. Mohammadian, Selective denitrogenation of model fuel through iron and chromium modified microporous materials (MSU-S), J. Environ. Chem. Eng. 5 (2017) 849–860.
[15] S.S. Meshkat, A. Rashidi, Z.H. Dastgerdi, M.D. Esrafili, Efficient DBT removal from diesel oil by CVD synthesized N-doped graphene as a nanoadsorbent: Equilibrium, kinetic and DFT study, Ecotoxicol. Environ. Saf. 172 (2019) 89–96, https://doi.org/10.1016/j.ecoenv.2019.01.042.
[16] M. Ahmaruzzaman, V.K. Gupta, Rice husk and its ash as low-cost adsorbents in water and wastewater treatment, Ind. Eng. Chem. Res. 50 (24) (2011) 13589–13613.

[17] T.A.H. Nguyen, H.H. Ngo, W.S. Guo, J. Zhang, S. Liang, Q.Y. Yue, Q. Li, T.V. Nguyen, Applicability of agricultural waste and by-products for adsorptive removal of heavy metals from wastewater, Bioresour. Technol. 148 (2013) 574–585.
[18] S.K. Sharma, A. Mudhoo, G. Jain, E. Khamis, Corrosion inhibition of Neem (Azadirachta indica) leaves extract as a green corrosion inhibitor for Zinc in $_{H}2S_{O}4$, Green Chem. Lett. Rev. 2 (1) (2009) 47–51.
[19] G. Pandhare, S.D. Dawande, Neem leaves powder as a low-cost adsorbent and its characteristics, Int. J. Adv. Eng. Technol. 4 (2) (2013) 61–62.
[20] M.B. Ibrahim, M.S. Sulaiman, S. Sani, Assessment of adsorption properties of neem leaves wastes for the removal of Congo Red and Methyl Orange, in: 3rd International Conference on Biological, Chemical & Environmental Sciences (BCES-2015) Sept. 21-22, (2015) Kuala Lumpur (Malaysia), 1-7. http://dx.doi.org/10.15242/IICBE.C0915067
[21] A. Sharma, K.G. Bhattacharyya, Azadirachta indica (Neem) leaf powder as a biosorbent for removal of Cd (II) from aqueous medium, J. Hazard. Mater. 125 (1-3) (2005) 102–112.
[22] A.A. Jinturkar, P.S.I. Sadgir, Removal of iron from aqueous solution using neem leaf powder as an adsorbent, Int. J. Innov. Res. Sci. Eng. Technol. (2017) 8948–8952.
[23] A. Ahmaruzzaman, S.L. Gayatri, A novel adsorbent for the removal of phenol, 4-nitrophenol, and 4- chlorophenol from aqueous solutions, J. Chem. Eng. Data 56 (7) (2011) 3004.
[24] G.B. Daware, A.B. Kulkarni, A.A. Rajput, Desulphurization of diesel by using low cost adsorbent, Int. J. Innov. Emerg. Res. Eng. 2 (6) (2015) 69–73.
[25] J. Wang, J. Wei, Selective and simultaneous removal of dibenzothiophene and 4-methyldibenzothiophene using double-template molecularly imprinted polymers on the surface of magnetic mesoporous silica, J. Mater. Chem. A 5 (2017) 4651–4659.
[26] Ihsanullah, F.A. Al-Khaldi, B. Abu-Sharkh, A.M. Abulkibash, M.I. Qureshi, T. Laoui, M.A. Atieh, Effect of acid modification on adsorption of hexavalent chromium (Cr(VI)) from aqueous solution by activated carbon and carbon nanotubes, Desalin. Water Treat. 57 (16) (2016) 7232–7244, https://doi.org/10.1080/19443994.2015.1021847.
[27] O.O. Sadare, M.O. Daramola, Adsorptive removal of dibenzothiophene from petroleum distillates using pomegranate leaf (*Punica granatum*) powder as a greener adsorbent, Chem. Eng. Commun. 206 (3) (2019) 333–345, https://doi.org/10.1007/s10904-019-01079-2.
[28] I. Langmuir, The constitution and fundamental properties of solids and liquids, J. Am. Chem. Soc. 38 (11) (1916) 2221–2295.
[29] M. Lam, Z. Ridzuan, Production of activated carbon from sawdust using fluidized bed reactor, in: International Conference on Environment, 2008 (ICENV 2008). Available at: https://core.ac.uk/download/pdf/11936677.pdf. (Accessed on 12_{th} December 2020)
[30] S. Lagergren, Zur theorie der sogenannten adsorption geloster stoffe, Kungliga Svenska Vetenskapsakademiens. Handlingar 24 (4) (1898) 1–39.
[31] Y.S. Ho, G. Mckay, Pseudo-second order model for sorption processes, Process Biochem. 34 (1999) 451–465.
[32] H. Patel, R.t. Vashi, A comparison study of removal of methylene blue dye by adsorption on neem leaf powder (NLP) and activated NLP, J. Environ. Eng. Landscape Manage. 21 (1) (2013) 36–41, https://doi.org/10.3846/16486897.2012.671772.
[33] C. Tsamo, A. Paltahe, D. Fotio, T.A. Vincent, W.F. Sales, One-, two-, and three-parameter isotherms, kinetics, and thermodynamic evaluation of Co(II) removal from aqueous solution using dead neem leaves, Int. J. Chem. Eng. 2019 (2019) 1–14, https://doi.org/10.1155/2019/6452672.
[34] K.R. Bharalia, G.K. Bhattacharyya, Kinetic and thermodynamic studies on fluoride biosorption by devdaru (polyalthia Longifolia) leaf powder, Oct. Jour. Env. Res. 2 (1) (2014) 22–31.
[35] C.M. Noorjahan, S.K. Jasmine, T. Deepika, S. Rafiq, Green synthesis and characterization of zinc oxide nanoparticles from neem (Azadirachta indica), Int. J. Sci. Eng. Technol. Res. 4 (2015) 5751–5753.
[36] M. Prabhu, S.R. Priscillia, K. Karitha, P. Manivasakan, V. Raj endian, P. Kulandaivelu, Invitro bioactivity and anti-microbial tuning of bioactive glass nanoparticles added with neem leaf powder. BioMed Res. Int. Article ID 950691 (2014) 1-10. http://dx.doi.org/10.1155/2014/950691.
[37] M.T. Ghaneian, B. Jamshidi, M. Dehvari, M. Amrollahi, Pomegranate seed powder as a new biosorbent of reactive red 198 dye from aqueous solutions: adsorption equilibrium and kinetic studies, Res. Chem. Intermed. 41 (5) (2015) 3223–3234.
[38] M.A. Al-Ghouti, M.A.M. Khraisheh, S.J. Allen, M.N. Ahmad, The removal of dyes from textile wastewater: a study of the physical characteristics and adsorption mechanisms of diatomaceous earth, J. Environ. Manag. 69 (3) (2003) 229–238.
[39] T. Santhi, S. Manonmani, T. Smitha, Removal of malachite green from aqueous solution by activated carbon prepared from the epicarp of Ricinus communis by adsorption, J. Hazard. Mater. 179 (1-3) (2010) 178–186.
[40] P. Saha, S. Chowdhury, S. Gupta, I. Kumar, R. Kumar, Assessment on the removal of malachite green using tamarind fruit shell as biosorbent, Clean Soil Air Water 38 (5-6) (2010) 437–445.
[41] M.K. Nazal, G.A. Oweimreen, MAZEN Khaled, M.A. Atieh, I. H. Aljundi, A.M. Abulkibash, Adsorption isotherms and kinetics for dibenzothiophene on activated carbon and carbon nanotube doped with nickel oxide nanoparticles, Bull. Mater. Sci. 39 (2) (2016) 437–450.
[42] V. Vadivelan, K.V. Kumar, Equilibrium, kinetics, mechanism, and process design for the sorption of methylene blue onto rice husk, J. Colloid Interf. Sci. 286 (1) (2005) 90–100.
[43] C. Namasivayam, N. Kanchana, R.T. Yamuna, Waste banana pith as adsorbent for the removal of rhodamine-B from aqueous solutions, Waste Manage. 13 (1) (1993) 89–95.
[44] I. Bettermann, C. Staudt, Desulfurization of kerosene pervaporation of benzothiophene/n-dodecane mixture, J. Membr. Sci. 343 (2009) 119–127.
[45] M. Ishaq, S. Sultan, I. Ahmad, H. Ullah, M. Yaseen, A. Amir, Adsorptive desulfurization of model oil using untreated, acid activated and magnetite nanoparticle loaded bentonite as adsorbent, J. Saudi Chem. Soc. 21 (2) (2017) 143–151.
[46] M. Ozacar, I.A. Sengil, Equilibrium data and process design for adsorption of disperse dyes onto Alunite, Environ. Geol. 45 (6) (2004) 762–768.
[47] W. Ahmad, I. Ahmad, M. Ishaq, K., Ihsan Adsorptive desulfurization of kerosene and diesel oil by Zn impregnated montmorollonite clay, Arabian J. Chem. 10 (2) (2017) S3263–S3269.
[48] A. Srivastav, V.C. Srivastava, Adsorptive desulfurization by activated alumina, J. Hazard. Mater. 170 (2-3) (2009) 1133–1140.
[49] C. Marín-Rosas, L.F. Ramírez-Verduzco, F.R. Murrieta-Guevara, G. Hernández-Tapia, L.M. Rodríguez-Otal, Desulfurization of low sulfur diesel by adsorption using activated carbon: adsorption isotherms, Ind. Eng. Chem. Res. 49 (9) (2010) 4372–4376.
[50] J. Gong, B. Wang, G. Zeng, C. Yang, C. Niu, Q. Niu, W. Zhou, Y. Liang, Removal of cationic dyes from aqueous solution using magnetic multi-wall carbon nanotube nanocomposite as adsorbent, J. Hazard. Mater. 164 (2009) 1517–1522.
[51] K. Yasemin, A.Z. Ayse, Adsorption characteristic of the hazardous dye Brilliant Green, Chem. Eng. J. 172 (2011) 199–206.
[52] M. Kumar, R. Tamilarasan, Kinetics, equilibrium data and modelling studies for the sorption of chromium by *Prosopis juliflora* bark carbon, Arabian J. Chem. 10 (supplement 2) (2017) S1567–S1577.